International Journal of
*Molecular Sciences*

MDPI

*Article*

# Preparation and Characterization of Poly(vinyl acetate-co-2-hydroxyethyl methacrylate) and In Vitro Application as Contact Lens for Acyclovir Delivery

**Saad Mohammed Alqahtani [1], Rana Salem Al Khulaifi [1], Mohammed Alassaf [1], Waseem Sharaf Saeed [1], Idriss Bedja [2], Amal Aldarwesh [2], Abeer Aljubailah [1], Abdelhabib Semlali [3] and Taieb Aouak [1,*]**

[1] Department of Chemistry, College of Science, King Saud University, Riyadh 11451, Saudi Arabia
[2] Department of Optometry, College of Applied Medical Sciences, King Saud University, Riyadh 11433, Saudi Arabia
[3] Groupe de Recherche en Écologie Buccale, Faculté de Médecine Dentaire, Université Laval, Quebec City, QC G1V 0A6, Canada
* Correspondence: taouak@ksu.edu.sa

**Abstract:** A series of poly(vinyl acetate-co-2-hydroxyethylmethacrylate)/acyclovir drug carrier systems (HEMAVAC) containing different acyclovir contents was prepared through bulk free radical polymerization of 2-hydroxyethyl methacrylate with vinyl acetate (VAc) in presence of acyclovir (ACVR) as the drug using a LED lamp in presence of camphorquinone as the photoinitiator. The structure of the drug carrier system was confirmed by FTIR and $^{1}$HNMR analysis, and the uniform dispersion of the drug particles in the carrier was proved by DSC and XRD analysis. The study of the physico-chemical properties of the prepared materials, such as the transparency, swelling capacity, wettability and optical refraction, was carried out by UV–visible analysis, a swelling test and measurement of the contact angle and the refractive index, respectively. The elastic modulus and the yield strength of the wet prepared materials were examined by dynamic mechanical analysis. The cytotoxicity of the prepared materials and cell adhesion on these systems were studied by LDH assay and the MTT test, respectively. The results obtained were comparable to those of standard lenses with a transparency of 76.90–89.51%, a swelling capacity of 42.23–81.80% by weight, a wettability of 75.95–89.04°, a refractive index of 1.4301–1.4526 and a modulus of elasticity of 0.67–1.50 MPa, depending on the ACVR content. It was also shown that these materials exhibit no significant cytotoxicity; on the other hand, they show significant cell adhesion. The in vitro dynamic release of ACVR in water revealed that the HEMAVAC drug carrier can consistently deliver uniformly adequate amounts of ACVR (5.04–36 wt%) over a long period (7 days) in two steps. It was also found that the solubility of ACVR obtained from the release process was improved by 1.4 times that obtained by direct solubility of the drug in powder form at the same temperature.

**Keywords:** poly(vinyl acetate-co-2-hydroxyethyl methacrylate); acyclovir; drug delivery; contact lenses



**Citation:** Alqahtani, S.M.; Al Khulaifi, R.S.; Alassaf, M.; Saeed, W.S.; Bedja, I.; Aldarwesh, A.; Aljubailah, A.; Semlali, A.; Aouak, T. Preparation and Characterization of Poly(vinyl acetate-co-2-hydroxyethyl methacrylate) and In Vitro Application as Contact Lens for Acyclovir Delivery. *Int. J. Mol. Sci.* **2023**, *24*, 5483. https://doi.org/10.3390/ijms24065483

Academic Editors: Marcel Popa and Silvia Vasiliu

Received: 24 February 2023
Revised: 10 March 2023
Accepted: 11 March 2023
Published: 13 March 2023



## 1. Introduction

Research in the field of drug delivery from polymer materials called "carriers" has been continuously developing for more than four decades [1–6]. Finding new drug delivery systems involving smart polymers capable of uniformly delivering a certain amount of drugs to achieve a prolonged therapeutic effect by uniformly and continuously releasing medication over an extended period of time is one of the challenges facing many researchers today. These drug delivery systems in the biomedical field involve one or more natural or synthetic polymers in the form of a blend or copolymers with desirable properties and one or more drugs. These systems create the ability to specifically target the point at which a drug is released in the body and/or the rate at which it is released. Poly(2-hydroxyethyl methacrylate) (PHEMA) belongs to the family of hydrogels. This stable and optically transparent polymer is considered as one of the most applied hydrogels in the field of

biomaterials. PHEMA-based hydrogels can be engineered to possess tissue-like water content and mechanical properties and exhibit excellent cyto-compatibility. This polymer is applied in several biomedical fields, including in contact lenses, wound dressings and drug delivery [7]. PHEMA is generally obtained by a radical polymerization route of 2-hydroxyethyl methacrylate. Since this polymer hydrogel is stable in vivo, its application in tissue engineering has been restricted. Several studies aimed to modify the properties of PHEMA to enhance the degree of hydration, degradation, mechanical properties and transport properties [8].

Poly(vinyl acetate) (PVAc) is a hydrophobic, biocompatible and biodegradable polymer (owing to the hydrolysable groups in the side chain). This polymer is also mainly synthesized by a free radical polymerization route and has also been applied in the biomedical domain, including in drug delivery, cell carriers and tissue engineering [9,10].

Several reports have highlighted the good biocompatibility of this polymer material in contact with blood, body fluids and tissues [10,11]. In an investigation reported in the literature [12], it was revealed that PVAc did not adsorb serotonin from platelet-free plasma and did not cause lysis of erythrocytes. PVAc is an inert polymer with the advantage that it does not induce a deleterious reaction in living tissue. In a histological study of embolized rat kidneys, it was revealed that there was no detectable damage in the vessel wall and no recanalization for up to 6 months. PVAc has also been shown to remain inert in the blood vessels [13]. Many patents have been filed on new compositions suitable for use in the embolization of blood vessels using materials based on biocompatible polymers comprising PVAc.

For example, the amount of serum albumin adsorbed by PVAc latex is considerably low, especially when the pH of the medium is between 5 and 8. This indicates the good compatibility of PVAc with blood [14], and this did not generate any procedural complication or thrombus formation on the electrodes of a PVAc catheter [15]. Many investigations have shown that PVAc also improves certain blood–polymer compatibility, thus, demonstrating the good blood compatibility of this polymer [16].

Despite the highly sought-after qualities of PVAc in the biomedical field, due to its hydrophobic nature, this polymer is not used alone as a carrier in drug delivery systems. In the most important research conducted in the field of drug delivery, PVAc has been used as a copolymer or blended with other polymers [17–20]. Indeed, Jannesari et al. [20] investigated a comparative study of the release of ciprofloxacin HCl (CipHCl) from PVAc and poly(vinyl alcohol) (PVA) used alone or as a blend to control the rate and drug release period in wound healing applications. The results obtained revealed that the PVA/PVAc mixture had useful and practical characteristics to meet these needs.

For example, the PVP-*block*-PVAc copolymer involving vinyl acetate and vinylpyrrolidone was used as a carrier by Bailly et al. [17] to improve the solubility of highly hydrophobic riminophenazine compounds. The "in vitro" experiments demonstrated that this drug carrier system exhibited no cytotoxicity and revealed the biocompatibility of the PVP-*block*-PVAc carrier system. The results obtained from this study indicate that this copolymer material could be a potential candidate as a carrier for hydrophobic drugs.

Acyclovir (ACVR) eye ointment is an important antiviral drug (structure in Scheme 1 and properties in Table 1) which, among others, treats eye infections caused by the herpes simplex virus (HSV), which causes symptoms such as redness, swelling, itching and tearing and which can cause corneal disease and vision loss [21,22]. This medicine works by preventing the virus from multiplying on the surface of the eyeball (cornea) by stopping the production of new virus and eliminating the infection in the eye. This medication works by killing the virus responsible for the infection and also prevents its multiplication.

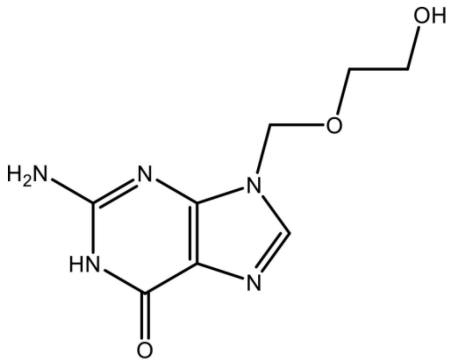


**Scheme 1.** Chemical structure of acyclovir (ACVR).

**Table 1.** Some physical–chemistry properties of acyclovir.

| Structure | $C_8H_{11}N_5O_3$ | Molar Mass | 225.208 g·mol$^{-1}$ |
|---|---|---|---|
| Density (g·mL) | 1.37 g·cm$^{-3}$ | Solubility in water | 1.30 mg·mL$^{-1}$ [23] [a] |
| Melting Temperature | 256.5 °C | $pKa_1$ and $pKa_2$ | 2.16 and 9.25 [23] [a] |

[a] Determined at 25 °C.

In this work, in order to control the amount of ACVR released by a contact lens based on PHEMA, controllable units of VAc (hydrophobic units) were incorporated in the chains of this hydrophilic polymer by copolymerization in order to reduce the swellability of this carrier, which is the main factor causing the release of excessive amounts of drug into the eyes.

To achieve this goal, contact lenses containing different amounts of ACVR were prepared by copolymerization of 2-hydroxyethyl methacrylate with vinyl acetate (HEMAVA) by the free radical polymerization route in presence of ACVR using LED light and camphorquinone as a photoinitiator. The structure of the prepared copolymer was characterized by FTIR and $^1$HNMR, and the dispersion of the ACVR particles in the copolymer matrix was characterized by DSC, XRD and SEM methods. The transparency, mechanical properties and the cytotoxicity were examined by UV–visible analysis, dynamic mechanical analysis and MTT methods, respectively. The "in vitro" ACVR release kinetics were followed by UV analysis, in which the effects of the drug contents in the HEMAVA, pH medium and the swelling capacity of the drug carrier systems were investigated.

## 2. Results

### *2.1. Characterization*

#### 2.1.1. FTIR Analysis

The FTIR spectra of virgin HEMAVA copolymer, ACVR and HEMAVAC composite with different compositions are gathered for comparison in Figure 1. As can be seen from the spectra of the copolymer and those of the composites, the total disappearance of the ethenic double bond (C=C) at 1638 and 1646 cm$^{-1}$, attributed to the HEMA and VAc monomers, respectively, indicates the formation of the HEMAVA copolymer. Although the ACVR content loaded in HEMAVA was minimal, small shifts in the absorption bands of hydroxyl groups from 3365.2 to 3373.5 cm$^{-1}$ and carbonyl groups from 1735.2 to 1731.0 cm$^{-1}$ were observed in the HEMAVAC spectra. This revealed the presence of different types of hydrogen bonds involving the different functional groups of the two components of the blend, as shown in Scheme 2.

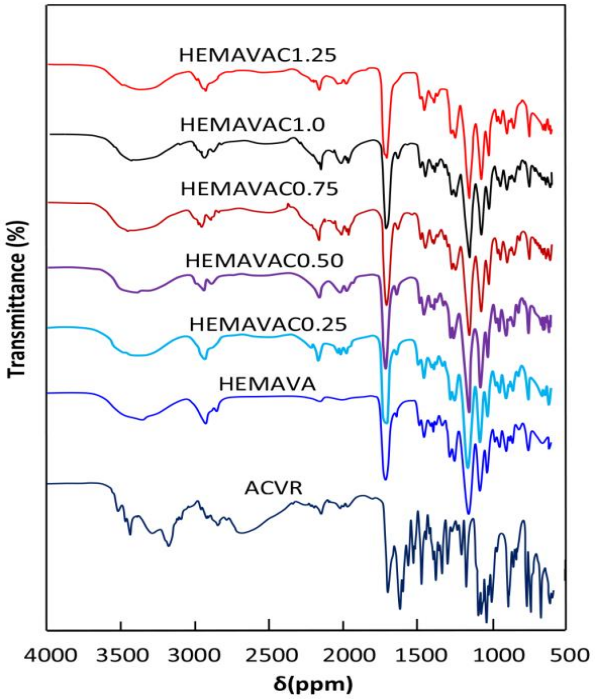


**Figure 1.** FTIR spectra of ACVR, virgin HEMAVA and HEMAVAC with different ACVR contents.

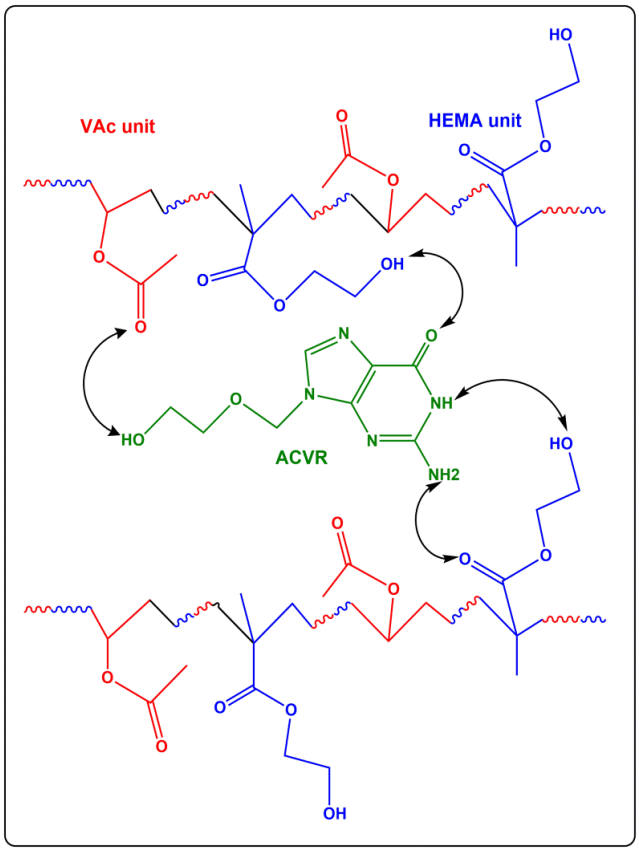


**Scheme 2.** Hydrogen bonds created between the different components of the HEMAVAC composites.

### 2.1.2. NMR Analysis

The $^{1}$HNMR spectra of ACVR, virgin HEMAVA and HEMAVAC with different ACVR contents are presented in Figure 2.

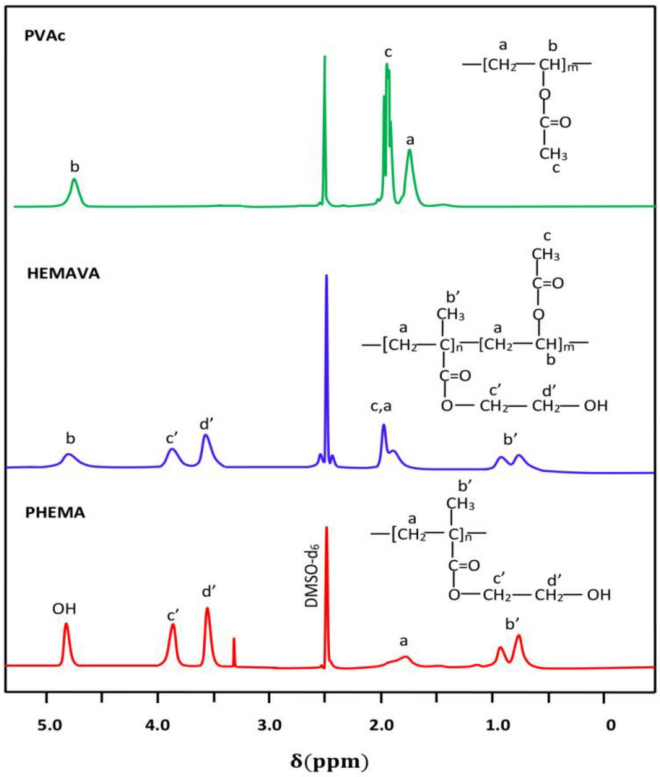


**Figure 2.** $^{1}$HNMR of PHEMA, PVAc homopolymers and HEMAVA copolymer.

The HEMAVA spectrum confirmed the formation of copolymer by the presence in its trace of all the signals characterizing the PHEMA and PVAc homopolymers and by the displacement of the signals of the ethylenic protons (a) of the vinyl acetate unit upwards of $\delta$. This chemical shift testified to the presence of a different ethylenic environment due to the new covalent bonds created between the two different monomeric units.

The composition in VAc and HEMA comonomers in the copolymer was estimated from the surface areas obtained by the integration of isolated signals located between 0.72 and 1.02 ppm, attributed to the three protons of the methyl ($b'$) of the HEMA units and that of the single proton ($b$) between 4.66 and 4.93 ppm belonging to the VAc unit in the copolymer, using Equation (1):

$$VAc(mol.\%) = \frac{A_b}{A_b + A_{b'}} 100, \quad (1)$$

where $A(b)$ and $A(b')$ are the surface areas of the signals ($b$) and ($b'$), respectively. The actual composition of VAc in the HEMAVA copolymer was taken from the average values calculated from the data deducted from the spectra of three samples, and the result obtained was 57.80 $\pm$ 0.32 mol.% of the VAc unit.

### 2.1.3. DSC Analysis

The DSC thermograms of the PVAc, PHEMA and HEMAVA copolymer are grouped in Figure 3. The curve profile of the synthesized HEMAVA shows a $T_g$ value at about 68 °C. This value is well located between those of its corresponding homopolymers (34 °C for PVAc and 85 °C for PHEMA). The $T_g$ value of this copolymer estimated from the Fox Equation (2) [24] was 56 °C, which deviated from the experimental value of 11 °C.

$$\frac{1}{Tg_{Cop}} = \frac{w_1}{Tg_1} + \frac{w_2}{Tg_2}, \quad (2)$$

where $w_i$ is the mass fraction of monomeric unit*i* in the copolymer, and $Tg_i$ is the glass transition temperature of the corresponding homopolymer. This deviation can be explained by the presence of inter-chain bonds in the copolymer, thus, limiting their sliding, and, consequently, such a phenomenon increased the $T_g$ value.

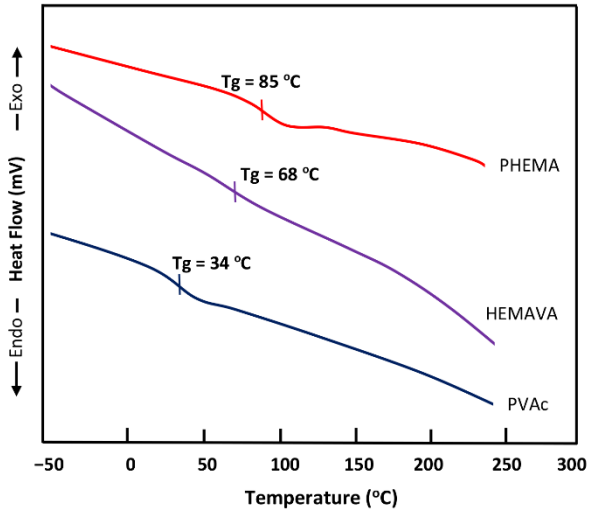


**Figure 3.** DSC thermograms of PVAc, PHEMA and HEMAVA.

The DSC thermograms of ACVR, virgin HEMAVA and loaded HEMAVAC with different ACVR contents are gathered in Figure 4. The amorphous nature of HEMAVA is proven by the absence of any endothermic peak belonging to an eventual fusion of this copolymer on its thermogram. The thermogram of the pure ACVR shows a melting temperature at 255 °C, which agrees with the literature [25,26]. Concerning the HEMAVAC composites, the disappearance of the endothermic peak on its thermal curve characterizing the fusion of this medication indicates that the ACVR drug is uniformly dispersed in the HAMAVA matrix at its molecular level. As can be also seen from these curve profiles, the $T_g$ value of the copolymer shifted toward the high temperatures when the ACVR loaded in the copolymer increased. This phenomenon can be explained by an increase in the intensity of the hydrogen bonds when the ACVR molecules insert themselves between the chains of the copolymer. This favors the reduction in chain slippage and, therefore, goes in the direction of an increase in the $T_g$ value of the copolymer. An increase in the ACVR content in the copolymer leads to an increase in the energy of the chains, and, consequently, this goes in the direction of increasing the value of the $T_g$.

#### 2.1.4. XRD Analysis

The XR diffraction patterns of ACVR, virgin HEMAVA and their HEMAVAC composites are collected for comparison in Figure 5. As can be seen from these data, the spectrum of the pure ACVR shows numerous distinct peaks localized at 6.8, 10.4, 16.7, 23.2, 26.0 and 29.1 2theta, indicating the crystalline character of this medication, which agrees with the literature [26]. However, the diffractogram of the copolymer exhibits two broad halos at 2θ = 17.07° and 21.11°, reflecting thus its amorphous structure because the appearance of broad peaks in this spectrum is due to the absence of finite-size, long-range crystallographic order. The copolymerization process may have interfered with the formation of any regular patterns in the HEMAVA sample. This seemed obvious because the presence in the copolymer of two units, each generating amorphous homopolymers [27,28], can only lead to an amorphous copolymer. Concerning the HEMAVAC composites, the total absence of ACVR signals on their diffractograms reveals that this medication is homogeneously dispersed at its molecular level in the HEMAVA matrix, thus, confirming the results obtained by the DSC analysis.

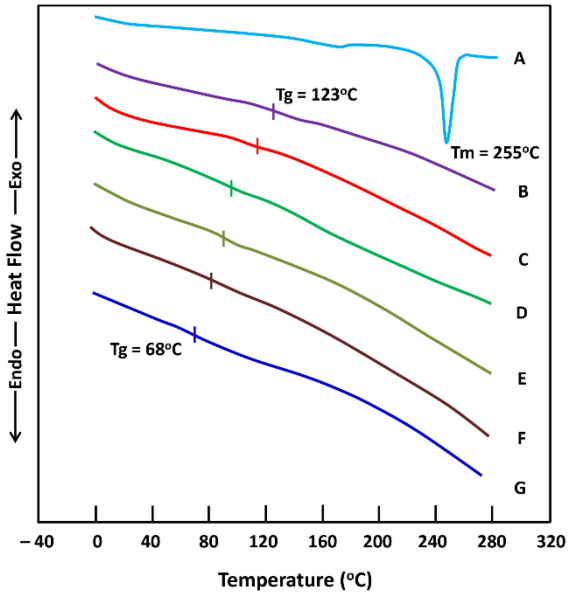


**Figure 4.** DSC thermograms of (**A**) ACVR; (**B**) HEMAVAC1.25; (**C**) HEMAVAC1.0; (**D**) HEMAVAC0.75; (**E**) HEMAVAC0.5; (**F**) HEMAVA0.25; and (**G**) virgin HEMAVA.

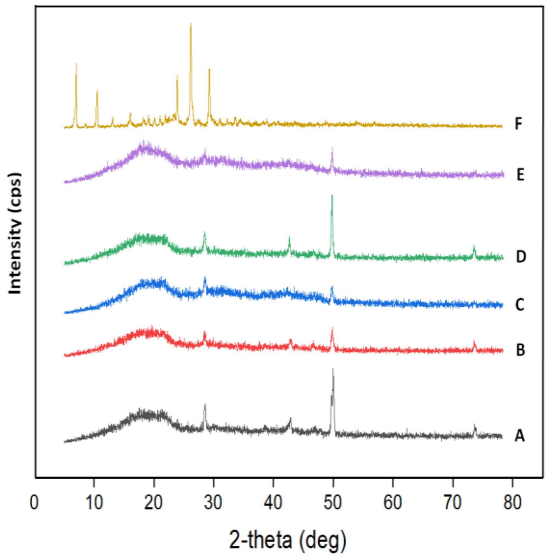


**Figure 5.** XRD patterns of (**A**) virgin HEMAVA; (**B**) HEMAVAC0.25; (**C**) HEMAVAC0.50; (**D**) HEMAVAC0.75; (**E**) HEMAVAC1.0; and (**F**) ACVR.

### 2.1.5. Swellability

The swelling capacity of any polymer used as carrier is an essential condition for performing the dynamic of a drug released from a drug carrier system. According to different investigators, this property is affected by different parameters such as the crosslink degree of the polymer [29,30], temperature [31,32] and pH medium in which the drug is released [33,34].

The variation of the swelling degree of virgin HEMAVA versus time is plotted in Figure 6. As can be seen from these data, the maximum swelling of this copolymer material is reached at about 13 h of the swelling process; during this period, 42.23 wt% of water is absorbed. Indeed, contact lens specialists suggest that the swelling capacity of contact lenses in water should ideally be between 30 and 40%. Swelling rates over 50% are high for this type of lens application because such a rate leads to drying of the eyes and leads to discomfort [35].

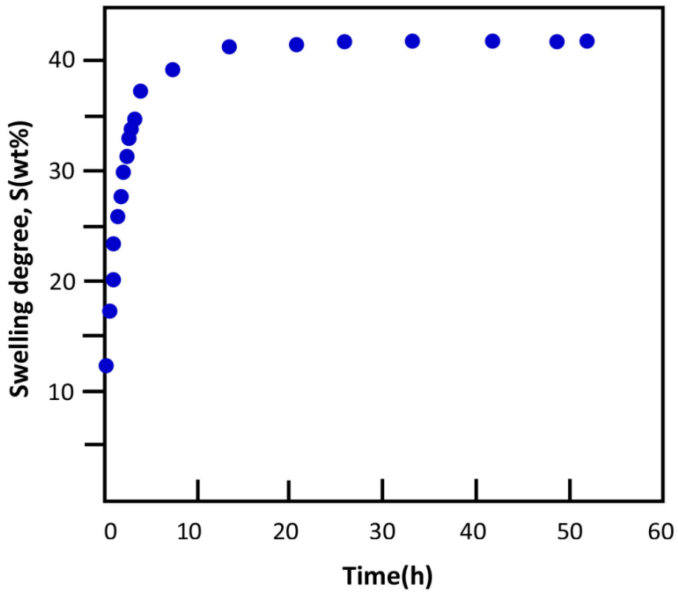


**Figure 6.** Variation of the swelling degree of HEMAVA in water at 37 °C.

2.1.6. Water Diffusion

According to Comyn [36], the kinetic that governs the diffusion of small molecules through a material, such as water through a polymer, is given by Equation (3):

$$\frac{w_t}{w_\infty} = 1 - \sum_{n=0}^{\infty} \frac{8}{(2n+1)^2\pi^2} exp\left[\frac{-D(2n+1)^2\pi^2 t}{l^2}\right], \quad (3)$$

where $w_t$ and $w_\infty$ are the mass of the sorbed molecules at time and at maximum absorption, respectively. $l$ and $D$ are the polymer film thickness and the diffusion coefficient, respectively. For the short times of the initial stage of diffusion, and when the $w_t/w_\infty$ ratio is lower than 0.5, Equation (4) takes the following reduced form:

$$\frac{w_t}{w_\infty} = 2\left(\frac{D}{\pi l^2} \times t\right)^{0.5}, \quad (4)$$

where $D$ is deducted from the slope of the linear portion of the curve corresponding to the variation of $w_t/w_\infty$ versus the square root of time. For the water/HEMAVA system, the curve profile of this polymer material, revealed in Figure 7, is a straight line with a $R^2$ = 0.9867. This indicates that the diffusion of water molecules through the HEMAVA matrix obeys Fick's model as long as the temperature of this polymer in media (37 °C) is well above *Tg* (68 °C). According to Massaro et al. [37], the basic equation of mass uptake by a polymer material is given by Equation (5):

$$\frac{w_t}{w_\infty} = kt^n, \quad (5)$$

where the exponent $n$ is the type of mechanism involved in the diffusion, and $k$ is a constant relating to the swelling rate, which, in turn, depends on the diffusion coefficient and the film thickness. By analogy with Equation (4), $n$ = 0.5, and $k$ takes the following expression: its value in this study is equal to 0.114 ± 0.005 $\mu m^{-0.5} \cdot s^{-0.5}$ deducted from the slope of the curve of this figure, and the diffusion coefficient calculated from Equation (6) is estimated at 14.167 $\mu m^2 \cdot s^{-1}$.

$$k = \frac{2}{l}\left(\frac{D}{\pi}\right)^{0.5}, \quad (6)$$

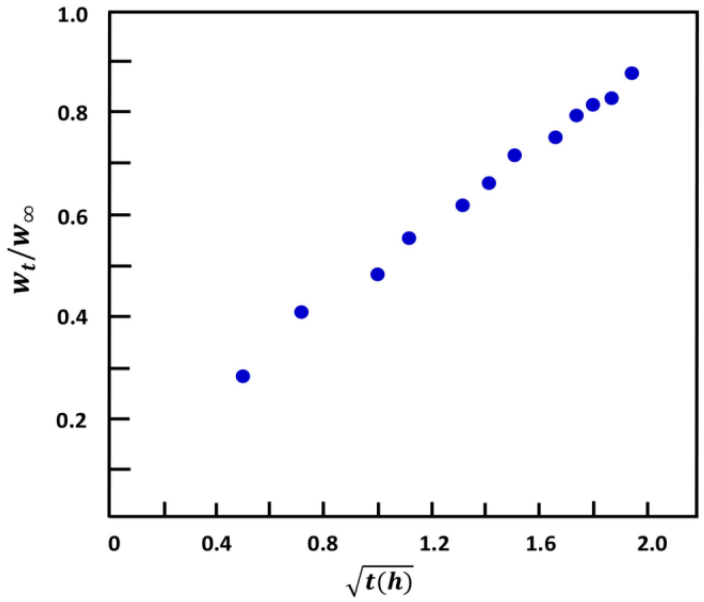


**Figure 7.** Variation of $w_t/w_\infty$ versus the square root of time of water sorbed at 37 °C through the HEMAVA matrix.

2.1.7. Mechanical Testing

The modulus of elasticity of the contact lens is closely related to the flexibility of a material. The modulus of elasticity characterizes the softness and fineness of the lens. The higher the modulus value, the more resistant the lens is against bending. The lower the modulus value, the more comfortable the lens is for its wearer, but the lens is less flexible and more fragile during handling. Contact lens material has a big impact on the modulus of elasticity. The more water the lens contains, the softer it is. The engineering tensile stress–strain curves of the prepared polymers, copolymers and drug carrier specimens obtained in this work are plotted in Figure 8, and the values of the apparent Young's modulus, E, deducted, are collected for comparison in Table 2. These data indicate an E value of 0.55 ± 0.13 MPa and a yield strength of 0.47 ± 0.12 MPa for the wet PHEMA and 15.02 ± 0.40 MPa and 29.30 ± 0.32 for PVAc, respectively, which are close to those values reported in the literature [38,39]. However, their wet HEMAVA copolymer material showed an apparent Young's modulus of 0.67 ± 0.13 MPa and yield strength of 0.80 ± 0.15 MPa. The incorporation of 57.80 mol.% VAc in the PHEMA chains slightly decreased the flexibility of this last material. On the other hand, the apparent Young's modulus of the HEMAVAC material increased slowly with the ACVR loaded in the copolymer in these investigated compositions' range. This indicates that the incorporation between 0.5 and 1.25 wt% of the ACVR in the HEMAVA matrix does not sensibly affect the flexibility of this carrier. The new material obtained took over mainly the mechanical properties of PHEMA, although it contained more PVAc units. This was mainly due to the effect of the equilibrium water content (EWC) and to the new rearrangement of a fraction of intra- and inter-chain hydrogen bonds during the passage from the OH ··· OH and OH ··· C=O bonds (HEMA–HEMA) to those of OH ··· C=O (HEMA–VAc). According to the literature [40], for soft contact lenses, the values of the elasticity modulus vary between 0.4 and 1.9 MPa. The comparison of the EWCs and the apparent Young's modulus with those of commercial lenses such as Tefilcon A, which are fabricated from PHEMA and manufactured by the Ciba Vision (Alcon) company (USA), indicated a good correlation with 38 wt% and 0.80 MPa, respectively. Other commercial lenses, such as Tetrafilcon A, produced by the CooperVision company (USA), are characterized by an equilibrium water content of 43 wt% and an apparent elasticity modulus of 0.60 MPa (measured central zone thickness (MCZT)). The diameter probe micrometer was measured with 10 mm [41].

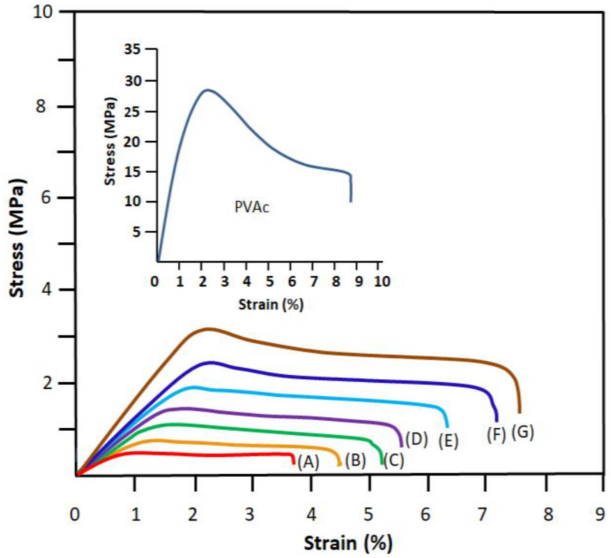


**Figure 8.** Engineering tensile stress–strain curves of PVAc, PHEMA (**A**), neat HEMAVA (**B**) and HEMAVAC containing 0.25 wt% (**C**), 0.50 wt% (**D**), 0.75 wt% (**E**), 1.0 wt% (**F**) and 1.25 wt% (**G**) ACVR contents.

**Table 2.** The apparent Young's modulus of the PHEMA, PVAc, HEMAVA and HEMAVAC with different ACVR contents.

| System | EWC (wt%) | Elastic Modulus (MPa) | Yield Strength (MPa) |
|---|---|---|---|
| PHEMA | 43.20 ± 0.21 | 0.55 ± 0.13 | 0.47 ± 0.12 |
| PVAc | - | 15.02 ± 0.40 | 29.30 ± 0.32 |
| HEMAVA | 42.23 ± 0.04 | 0.67 ± 0.13 | 0.80 ± 0.15 |
| HEMAVAC0.25 | 42.45 ± 0.05 | 0.82 ± 0.14 | 1.05 ± 0.18 |
| HEMAVAC0.50 | 43.16 ± 0.05 | 0.94 ± 0.15 | 1.40 ± 0.20 |
| HEMAVAC0.75 | 49.85 ± 0.04 | 1.05 ± 0.17 | 1.92 ± 0.25 |
| HEMAVAC1.00 | 63.86 ± 0.04 | 1.25 ± 0.19 | 2.27 ± 0.22 |
| HEMAVAC1.25 | 81.80 ± 0.04 | 1.50 ± 0.20 | 3.10 ± 0.23 |

#### 2.1.8. Transparency

The transparency of the wet PHEMAVAC specimens containing different ACVR contents was examined directly by ocular vision and supported by UV–visible analysis. As can be seen from the photos in Figure 9, all the specimens had an appearance that was transparent, colorless and homogeneous. The results of the UV–visible analysis of these specimens in the wavelength range 400–800 nm, as shown in Figure 10, well supported these observations. Table 3 summarizes the transmittance values of visible light through these samples. As can be observed through these data, the virgin specimen showed an average percentage transmittance of 89.54% when the wavelength (λ) varied from 400 to 800 nm, while those loaded with different amounts of ACVR were characterized by more than 76.90%, and the maximum transparency was obtained for the contact lens containing 0.25 wt% ACVR with 86.49% transmittance, which are in the range of the contact lens parameters reported in the literature [42].

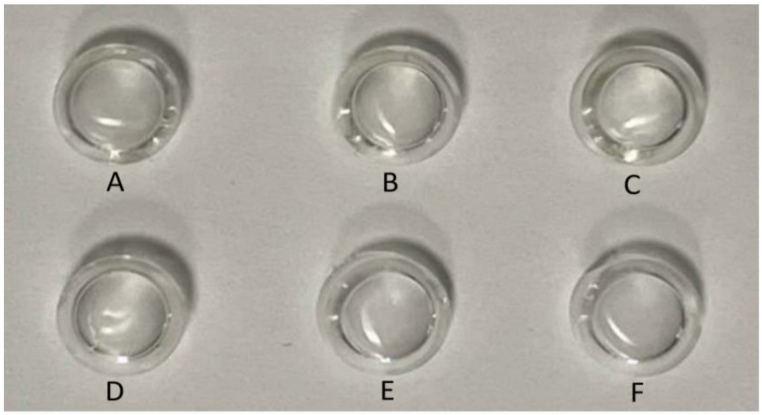


**Figure 9.** Photos indicating the transparency of the contact lenses: (**A**) virgin HEMAVA; (**B**) HEMAVAC0.25; (**C**) HEMAVAC0.50; (**D**) HEMAVAC0.75; (**E**) HEMAVAC1.00; (**F**) HEMAVAC1.50.

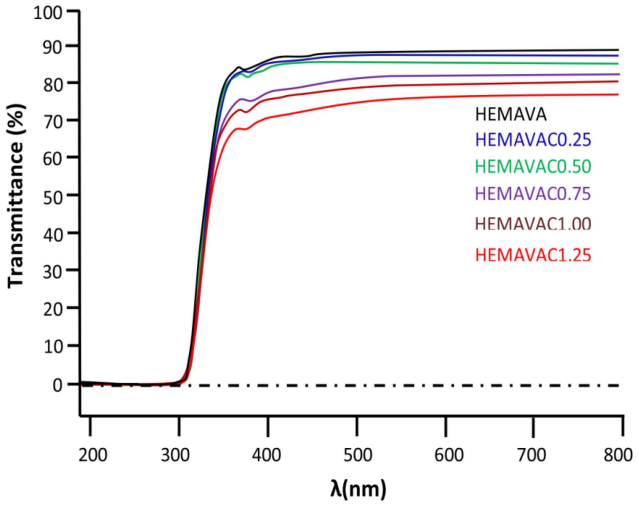


**Figure 10.** UV–visible spectra of virgin HEMAVA and HEMAVAC containing different ACVR contents.

**Table 3.** Percentages of the visible light transmittance of virgin HEMAVA and HEMAVAC with different ACVR contents.

| System | Transmittance (%) | Absorbance (%) | Reflectance (%) |
|---|---|---|---|
| HEMAVA | 89.51 ± 0.34 | 0.049 ± 0.012 | 10.441 ± 0.012 |
| HEMAVAC0.25 | 86.49 ± 0.23 | 0.059 ± 0.009 | 13.451 ± 0.016 |
| HEMAVAC0.50 | 86.49 ± 0.38 | 0.060 ± 0.009 | 18.450 ± 0.021 |
| HEMAVAC0.75 | 81.51 ± 0.32 | 0.096 ± 0.007 | 18.394 ± 0.022 |
| HEMAVAC1.00 | 80.51 ± 0.24 | 0.089 ± 0.007 | 19.986 ± 0.021 |
| HEMAVAC1.50 | 76.90 ± 0.27 | 0.114 ± 0.008 | 22.986 ± 0.023 |

### 2.1.9. Refractive Indices

The determination of the optical refractive index is essential in the characterization of a material for potential use as contact lenses in the medical field. According to Varikooty et al. [38], a relatively high refractive index can reduce the lens thickness and, thereby, significantly improves the wearer's comfort. Thus, the refraction indices of the prepared specimens were evaluated by measuring the refraction of the light in each prepared polymer and copolymer material, and the results obtained are gathered for comparison in Table 4. As can be seen from these data, no sensible change in the refractive index was observed when changing the composition in ACVR in the HEMAVAC material. The values of the refractive index for PHEMA and PVA copolymers obtained in this work, which were 1.4360

and 1.4669, respectively, agreed with those of the literature for comparable materials [43,44]. On the other hand, the refractive index of virgin HEMAVA and HEMAVAC varied from 1.4301 to 1.4526 when the wavelength passed from 405 to 670 nm. These values are comparable to those of commercial soft contact lenses, which vary from 1.40 to 1.43 [45]. As can be also seen from these data, a slight shift toward the low refractive index was observed when the ACVR content in the HEMAVA matrix increased. This confirmed that the ACVR was really uniformly dispersed in the copolymer matrix in its molecular state, because the presence of eventual, aggregated ACVR particles incrusted in the copolymer matrix can easily deviate or reflect the optical path of the laser beam, which was not the case here.

**Table 4.** The refractive index values measured for PHEMA, PVAc, HEMAVA and HEMAVAC with different ACVR contents.

| Specimen | Refractive Index Measured at 37 °C | | |
|---|---|---|---|
| **Λ (nm)** | **405** | **532** | **670** |
| PHEMA | 1.5220 | 1.5125 | 1.4817 |
| PVAc | 1.3872 | 1.3465 | 1.2804 |
| HEMAVA | 1.5026 | 1.5003 | 1.4314 |
| HEMAVAC0.25 | 1.5025 | 1.4901 | 1.4312 |
| HEMAVAC0.50 | 1.5023 | 1.4895 | 1.4308 |
| HEMAVAC0.75 | 1.4998 | 1.4887 | 1.4305 |
| HEMAVAC1.00 | 1.4956 | 1,4884 | 1.4303 |
| HEMAVAC1.25 | 1.4948 | 1.4880 | 1.4301 |

2.1.10. Wettability

The wettability of virgin and loaded HEMAVA film samples was evaluated from the water contact angle measurements in air at ambient temperature (25 °C), and the images obtained are gathered in Figure 11. As can be seen from the data of Table 5, a slight shift toward the high values of the measured optical contact angle was observed when the ACVR was added to the HEMAVA material. This value increased slowly when the drug loaded in this copolymer material increased. This indicates that the wettability of this specimen increased slowly when the drug loaded in the HEMAVAC system increased from 0.25 to 1.50 wt%. This went in the same direction as the relation that existed between the elastic modulus and the EWC previously shown in Table 2. In this contact angle range, all these materials were considered as partially wettable [46]. The increase in the wettability of the HEMAVAC material was probably due to the increase in the density of inter-chain interactions of the hydrogen bond type involving the $-NH_2$, $-OH$ and $-C=O$ groups of the ACVR molecules and the $-OH$ and $-C=O$ groups of copolymers because the incorporation of hydrophil molecules, such as ACVR, in a moderately hydrophil polymer matrix, such as HEMAVA, leads to an increase in the hydrophil behavior of the resulting material. Therefore, this leads to an increase in the affinity of water molecules toward the resulting material. In a study carried out by Toledo et al. [47] on the influence of magnetic field on the physical–chemical properties of liquid water, it was revealed that the competition between the different hydrogen bonds (intra- and intermolecular) gives rise to the weakening of intra-cluster hydrogen bonds in water, forming smaller cluster with stronger inter-cluster hydrogen bonds. In our context, this phenomenon seems to confirm our explanation.

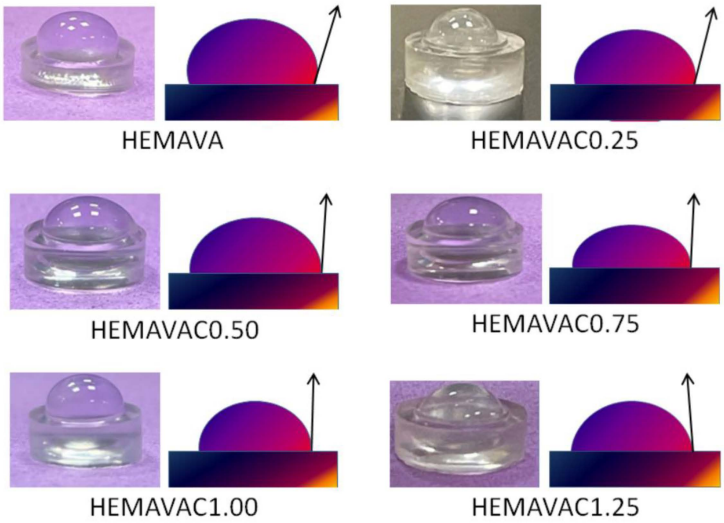


**Figure 11.** Contact angle measurements of virgin HEMAVA and HEMAVAC with different ACVR contents.

**Table 5.** The contact angles values of virgin HEMAVA and HEMAVAC with different ACVR contents.

| System | Contact Angle (Degree) |
|---|---|
| HEMAVA | 76.30 |
| HEMAVAC0.25 | 77.45 |
| HEMAVAC0.50 | 78.03 |
| HEMAVAC0.75 | 85.50 |
| HEMAVAC1.00 | 88.00 |
| HEMAVAC1.25 | 94.20 |

2.1.11. SEM Analysis

The surface morphologies of ACVR powder, virgin HEMAVA and HEMAVAC with different ACVR contents before and after the release process were examined by the SEM technique, and the micrographs of the HEMAVAC0.25 and HEMAVAC1.25 systems and those of their pure components taken as examples are shown for comparison in Figure 12.

As can be observed from the image (A), the ACVR particles showed a crystalline structure in the lamellae form of different dimensions (1.23–26.3 μm) deposited one on the other. The virgin HEMAVA film shown on the micrograph (B) had a smooth and homogeneous surface devoid of any particles extra to the two components of the material, such as dust, for example. The surface morphologies of HEMAVAC0.25 (image C) and HEMAVAC1.25 (image E), which contained 0.25 and 1.25 wt% ACVR contents, respectively, showed, before the release process, a smooth and gently wavy surface devoid from any traces of aggregated ACVR particles. This also confirms the results obtained by the DSC and XRD analyses, which revealed that this medication is dispersed in the HEMAVA matrix at its molecular level.

The images on the right (D and F) show rough surfaces containing a high density of micro-pores uniformly dispersed on the surface of the specimens, thus, revealing that a large amount of ACVR was released into the medium during the entire period of the release process.

As can be seen from the comparison of these two photos, in the sample that contained the most drugs (HEMAVAC1.25), the pores left by the jettison appeared larger than those of HEMAVAC0.25. This also testifies to the highest rate of ACVR released during the process.

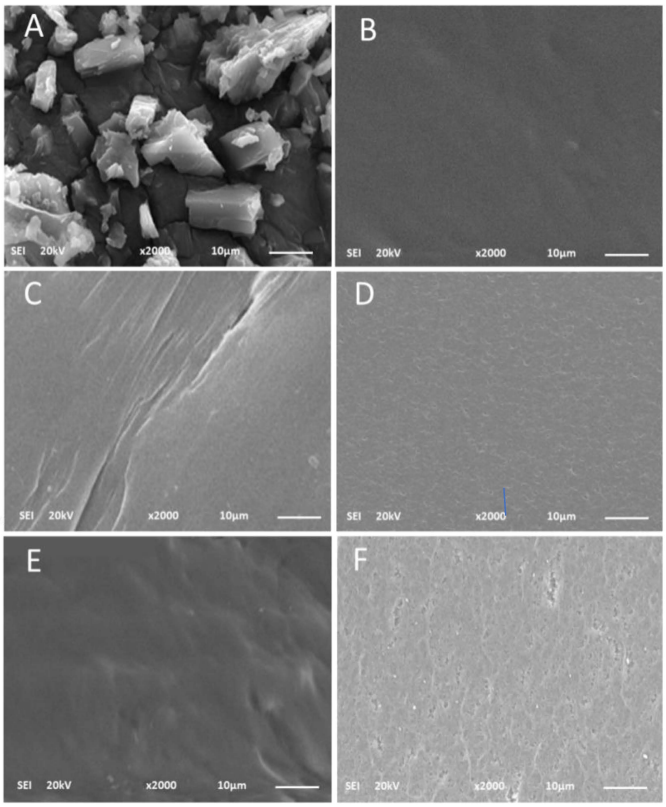


**Figure 12.** SEM images of: ACVR powder (**A**); HEMAVA film sample (**B**); HEMAVAC0.25 film sample before (**C**) and after (**D**) the release process; HEMAVAC1.25 film sample before (**E**) and after (**F**) the release process.

### 2.1.12. Cell Viability and Cell Adhesion

The results of the cell toxicity test obtained at 490 nm for the virgin HEMAVA and HEMAVAC drug carrier systems using the LDH assay are shown in the histogram in Figure 13. As shown by these data, the virgin HEMAVA appears to be non-toxic for normal gingival epithelial cells, and the incorporation between 0.25 and 1.25 wt% of ACVR in these biomaterials did not have a significant effect on their viability. The increase in cell toxicity from 37 to 59.3% when the ACVR content increased in the drug carrier system was probably due to the effect of the very active antiviral medication on the cell viability.

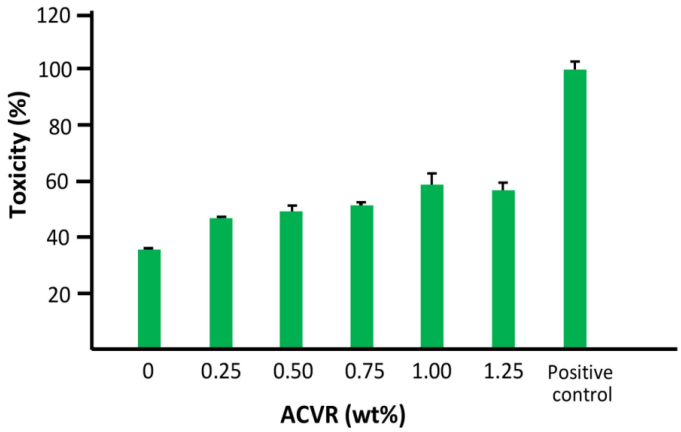


**Figure 13.** Effect of HEMAVAC drug carrier systems with different ACVR contents on human epithelial cell toxicity using LDH assay. The positive control was the collagen membrane (collapse) (adhesion 100%).

The results of the percentage of cell adhesion on the virgin HEMAVA and HEMAVAC specimens examined by the standard MTT test are shown in a histogram in Figure 14. As can be observed from these data, a significant cell adhesion rate compared to the negative control was observed for any ACVR/HEMAVA ratio in the drug carrier system. The absorbance at 550 nm increased more than four times with the virgin specimen compared to that without cells, while a non-significant difference was observed when the ACVR was incorporated in the HEMAVA matrix.

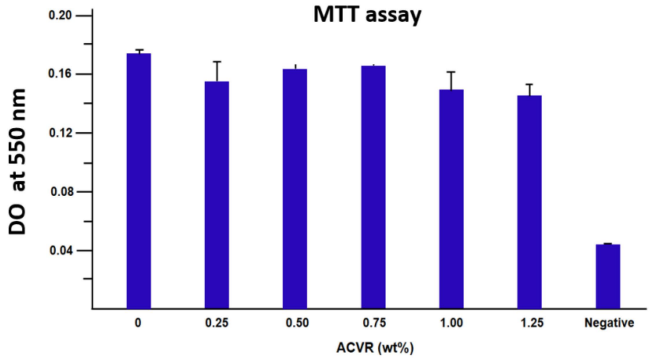


**Figure 14.** Cell adhesion on the virgin HEMAVA and HEMAVAC specimens with different ACVR contents. The error bars correspond to the standard deviation between the minimal and the maximal values which were obtained from the three experiments carried out.

### *2.2. In Vitro Release Dynamic of ACVR*

#### 2.2.1. Kinetic Release of ACVR

The in vitro release of ACVR from the HEMAVAC drug carrier systems was monitored at 37 °C for one week in a neutral pH medium, and the cumulative percentage of medication released was determined according to Equation (7):

$$R\ (wt\%) = \frac{m_t}{m_0} \times 100, \quad (7)$$

where $m_0$ and $m_t$ are the initial mass and the mass released in the medium at $t$ time, respectively. The variation of the cumulative ACVR released from the HEMAVAC systems versus time is plotted in Figure 15. The profiles of the curves obtained show a logarithmic growth of the percentage of ACVR released over time. During one week, between 8.90 and 41.90 wt% of the total amount of drug loaded was released. These patterns also reveal that between 85 and 90 wt% of ACVR was released during only the first five hours, depending on the VAc content in the HEMAVAC systems.

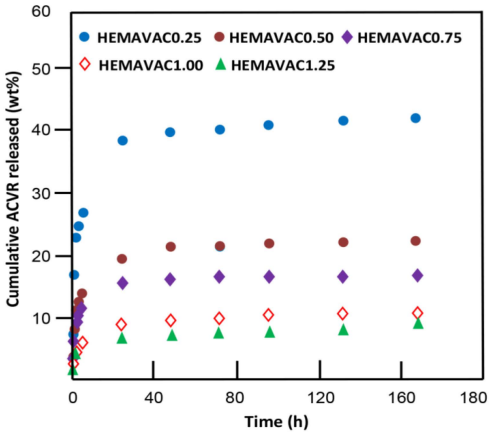


**Figure 15.** Variation of the cumulative ACVR released from the HEMAVAC systems vs. time.

This phenomenon could be due to the contribution of two main factors; the first one is physical, which is the dissolution of the ACVR particles stuck or slightly embedded on the surface of the film sample, and the second is thermodynamic, which is the large difference between the free enthalpy of dissolution ($G_d$) inside and outside of the polymer matrix during this period until equilibrium was reached, which was characterized by a zero release.

$$\Delta G_d = G_d(inside) - G_d(outside) = 0$$

#### 2.2.2. ACVR Solubility Improvement

The solubility of any medication in an aqueous medium is a determinant factor that governs the rate and the dynamics of its absorption by target organs. According to the literature, the solubility of pure ACVR powder in water is estimated at 1.30 mg·mL$^{-1}$ at 25 °C [23]. It is well known that, for poorly water-soluble drugs, the smaller the size of the dispersed particles, the greater their solubility [38,44,48]. Indeed, when the size of the drug particles decreases, this leads to an increase in their total surface area, thus, leading to an increase in the number of contacts between the drug and the water molecules. This promotes an increase in the dissolution of a very large number of particles, particularly when they are slowly released into water at their molecular level. In this work, the maximum solubility of ACVR in water obtained at 37 °C was estimated through the cumulative amount of this drug released until equilibrium, and the result obtained was 2.70 mg·mL$^{-1}$. This value represents 1.42-fold that of the solubility determined in this work in the same temperature by direct dissolution of this medication as powder, which was 1.90 mg·mL$^{-1}$.

#### 2.2.3. Diffusion Behavior of ACVR through HEMAVAC System

In order to identify the release dynamic of ACVR in the HEMAVAC drug carrier system through the release process, the diffusion behavior of this medication was investigated. As shown by the data plotted in Figure 15, for any ACVR/HEMAVA composition, the ACVR released from these drug carrier systems did not exceed 60 wt% of the total amount of this medication initially loaded in the HEMAVA matrix. Therefore, the Fick model is applicable to describe the diffusion of acyclovir from these drug carrier systems. In these conditions, the diffusion coefficient of ACVR ($D_{ACVR}$) through the HEMAVAC material is given by Equation (8) [49–54]:

$$D_{ACVR} = \frac{0.198 \times d^2}{t} \times \left[\frac{m_t}{m_o}\right]^2, \quad (8)$$

where $d$ is the thickness of the film sample. The $D_{ACVR}$ value is determined when the permanent regime is reached, and, therefore, all ACVR particles deposed or pressed on the film surface are completely removed by washing in water. In these conditions, the curve profiles of $D_{ACVR}$ versus time are meaningful and reflect the dynamics of ACVR released in the media inside the polymer matrix. The variation of $D_{ACVR}$ through the HEMAVAC drug carrier systems versus the inverse of time, calculated from the data of Figure 15 and Equation (8), is plotted in Figure 16. As shown from these curve profiles, straight lines were obtained for each HEMAVAC system. This indicates that the diffusion of ACVR through these drug carrier systems follows the Fickian model. These results also indicate that the permanent regime of the dynamic release was reached. In light of these findings, it was possible to determine the second stage of the release process, which is generally localized between 2 and 7 days.

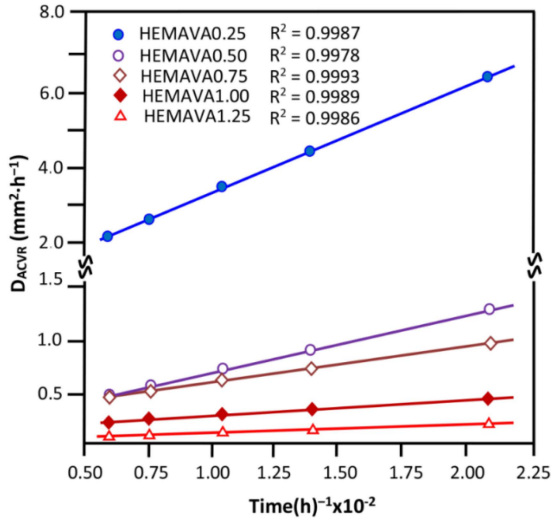


**Figure 16.** Variation of the diffusion coefficient of ACVR through the HEMAVAC drug carrier systems containing different ACVR contents versus the inverse of time.

### 2.2.4. Effects of the ACVR Content

The effect of the ACVR content incorporated in the HEMAVAC drug carrier system on the release dynamic of this medication was studied during 24, 48 and 72 h of the release process, and the results obtained are plotted in Figure 17.

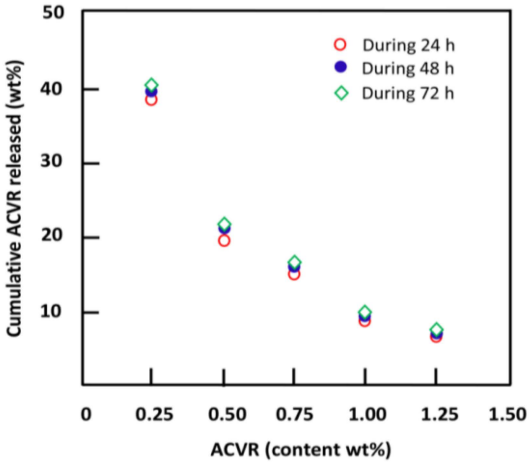


**Figure 17.** Variation of the cumulative ACVR released from HEMAVAC drug carrier systems during 24, 48 and 72 h versus the ACVR content.

The profile of these curves shows that the release dynamic of ACVR followed practically the same pattern for all time-points, at which the cumulative drug released dramatically decreased following logarithmic curves. In terms of percentage amount released, the highest ACVR release was reached when the initial amount of ACVR filled in the HEMAVA matrix was 0.25 wt%, and the lowest was reached with 1.25 wt% load. This is closely related to the limit solubility of ACVR in water inside the polymer carrier. So, whatever the amount of ACVR loaded into the polymer matrix, only a maximum of 2.70 mg/mL of this drug dissolves inside the HEMAVA carrier and is then released in the medium. When the amount of ACVR incorporated into the system is less than or close to this solubility, the percentage of ACVR released is higher (the case for HEMAVAC0.25). On the other hand, when the amount of this medication initially loaded in the polymer carrier is much higher, this percentage is lower (the case for HEMAVAC1.25).

The drug release dynamic from a drug carrier system does not depend only on the nature and structure of polymer used as carrier but also on the water–drug solubility

and its swellability. Several authors intensively investigated these factors [14,29,50–58]; however, the explanations suggested by those researchers still remain unconvincing due to the multiple parameters that simultaneously intervene in the release process. In this work, the effect of the swelling capacity of the HEMAVAC material on the release dynamic of ACVR in neutral pH medium was studied, and the results obtained are summarized in Table 6. As can be seen from these data, the ACVR released from this drug carrier system decreased when the EWC increased. Similar results were also obtained by Wan et al. [55] using an ibuprofen-crosslinked hydroxypropyl methylcellulose drug carrier system. On the other hand, in an investigation reported by Khalid et al. [56] on a lactulose-crosslinked poly(methyl methacrylate-co-itaconic acid) drug carrier system, quite the opposite was obtained, and the release dynamic of lactulose increased with the swelling capacity of this copolymer. These contradictory observations can be explained by the two antagonistic factors, evoked in the previous section, which intervene simultaneously. On the one hand, a more important swelling goes in the direction of increasing the amount of ACVR dissolved in water leading to a higher release dynamic, and, on the other hand, a lower solubility of the medication in water limits its dissolution and, consequently, leads to lower release dynamics. When the phenomenon of solubility predominates, a reduction in the dynamics of release takes place in the process.

**Table 6.** Effect of the EWC on the release dynamic of ACVR at 72 h of the release process.

| System | ACVR Content (wt%) | EWC (wt%) | Cumulative ACVR Released (wt%) |
|---|---|---|---|
| HEMAVAC0.25 | 0.25 | 42.45 | 40.32 |
| HEMAVAC0.50 | 0.50 | 43.16 | 21.64 |
| HEMAVAC0.75 | 0.75 | 49.85 | 16.32 |
| HEMAVAC1.00 | 1.00 | 63.86 | 9.89 |
| HEMAVAC1.25 | 1.25 | 81.80 | 7.52 |

Through these results, it was found that the percentage of ACVR released dropped by 5.36 times when the swelling rate of the material doubled. This seems to contradict what was to happen; because the greater the quantity of water which penetrates in the drug carrier system is important, the greater the dissolution of the particles of drug and the greater the dynamics of its release in the medium. This contradiction can only be removed by the solubility limit of ACVR in the system, thus, confirming the results obtained in the previous section, in which the cumulative ACVR released dramatically decreased when the initial drug loaded in the copolymer matrix increased five times.

#### 2.2.5. Performance of the HEMAVAC Drug Carrier System

The performance of the HEMAVAC drug carrier system was evaluated in this study from the data of the instantaneous release rates of ACVR, which were obtained from the slopes of the pseudo-linear portions of the kinetic curves shown in Figure 15. As can be seen from these curve profiles, practically two main stable zones can be observed for each ACVR/HEMAVA composition, and their release characteristics are grouped in Table 7. The first zone, observed during the first day of the release process, in which 5.51–36.0 wt% ACVR was released with a release rate of 0.83–6.03 wt%·h$^{-1}$, depending on the drug content loaded in the HEMAVA carrier, was short. This step was followed by a larger zone (6 days), which extended until the end of the release process. During this period, 2.5–4.02 wt% of cumulative ACVR was slowly and uniformly released in this neutral pH medium with a release rate of 0.02–0.03 wt%·h$^{-1}$ depending on the ACVR incorporated in the HEMAVA matrix. The large amount of ACVR released during the first period has already been explained in Section 2.2.1.

**Table 7.** Stable zones and instantaneous release of ACVR from the HEMAVAC drug carrier system with different ACVR contents.

| Drug Carrier System | Stable Zone (h) | ACVR Released (wt%) | Release Rate (wt%·h$^{-1}$) |
|---|---|---|---|
| HEMAVAC0.25 | 0–6 | 36.10 ± 0.06 | 6.03 ± 0.01 |
| | 24–168 | 04.50 ± 0.01 | 0.03 ± 0.02 |
| HEMAVAC0.50 | 0–6 | 20.00 ± 0.02 | 3.33 ± 0.01 |
| | 24–168 | 02.50 ± 0.03 | 0.02 ± 0.03 |
| HEMAVAC0.75 | 0–6 | 12.00 ± 0.02 | 2.03 ± 0.02 |
| | 24–168 | 03.03 ± 0.03 | 0.02 ± 0.02 |
| HEMAVAC1.00 | 0–6 | 06.20 ± 0.01 | 1.10 ± 0.02 |
| | 24–168 | 04.02 ± 0.03 | 0.03 ± 0.01 |
| HEMAVAC1.25 | 0–6 | 05.04 ± 0.03 | 0.83 ± 0.02 |
| | 24–168 | 03.51± 0.03 | 0.02 ± 0.04 |

It is well known that the eye and its surroundings only absorb a tiny amount of drug. To target the delivery of a certain amount of drug through the ocular surface, there is no other way than to prolong its residence time on this surface.

Regarding the relationship that exists between the structure of the HEMAVAC system and the release dynamics of ACVR, the uniform distribution of this medication in the HEMAVA matrix makes it possible to obtain a material combining several parameters required to meet the optimum conditions for its application as a drug contact lens system. Indeed, the incorporation of VAc hydrophobic units in the PHEMA chains and the addition of ACVR molecules to the copolymer obtained allows a redeployment of the interaction forces of the inter- and intramolecular hydrogen bonds, which is favorable for the absorption of adequate amounts of water molecules, allowing uniform and controlled medication over a long period of time.

## 3. Materials and Methods

### *3.1. Chemicals*

2-hydroxyethylmethacrylate (HEMA) (purity, ≥99%), vinyl acetate (Vac) (purity, ≥99%) and camphorquinone (CQ) (purity, 97%) were provided by Sigma Aldrich (Merck, Germany). Acyclovir (Zovirax 800 mg) (ACVR) tablet was purchased from Riyadh Pharma (Riyadh, Saudi Arabia). Monomers were purified by distillation under reduced pressure and stored under nitrogen gas before use. Photoinitiator was used without purification. An 800 mg amount of Zovirax was finely ground using a ceramic mortar and then dissolved in the monomer mixture. The solution obtained was then filtered from the solid residues on Whatman 01 filter paper. The human epithelial cell line (HECL) GMSM-K, constructed by Gilchrist et al. (2000), was provided by Dr. Grenier of Université Laval. Dulbecco's Modified Eagle's Medium (DMEM) was purchased from Corning, Manassas, VA, USA. Fetal bovine serum (FBS) was provided by Gibco (New York, NY, USA), and 1% penicillin/streptomycin solution was purchased from Sigma Aldrich (St. Louis, MO, USA). Lactate dehydrogenase (LDH) detection kit was obtained from BioVision (BioVision, Milpitas, CA, USA).

### *3.2. Preparation of Poly(2-hydroxy ethylmethacrylate-co-vinyl acetate) (HEMAVA)*

HEMAVA containing 58 mole of vinyl acetate unit was synthesized by free radical polymerization route of HEMA with VAc in two ways by radiation using LED method. A 12.84 g (0.098 mol.) amount of HEMA and 19.82 g (0.230 mol.) of VAc were mixed together while stirring, then 0.055 g of CQ used as photoinitiator was added to the monomer mixture. The reaction mixture was deposed in a Teflon cylindric molder inside the reactor of Scheme 3. A moderate stream of nitrogen gas (3 mL/min) passed through the reactor throughout the polymerization period, as shown in this scheme. The polymerization reaction was carried out by radiation of LED light at 60 °C, and the polymer obtained was easily detached from the mold and was dried in the open air for 12 h then in a vacuum

oven at a temperature of 40 °C for 12 h. The material obtained was a thin, transparent and flexible circular pallet.

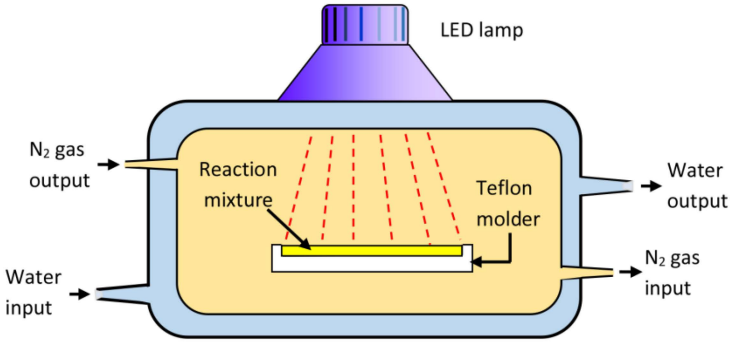


**Scheme 3.** Reactor used in the photo-copolymerization of HEMA with VAc.

### 3.3. Preparation of HEMAVAC Composite

A known amount of ACVR was dissolved while stirring in a mixture containing HEMA and VAc monomers and CQ until complete dissolution. The assembly was placed in a mold then placed in the reactor, and the copolymerization occurred in the same conditions described previously in Section 2.1. A series of HEMAVAC film composites with different ACVR contents was prepared, and the experimental conditions are gathered in Table 8.

**Table 8.** Preparation conditions of HEMAVA/ACVR drug release system.

| Drug Carrier System | HEMA (g) | Vac (g) | CQ (g) | ACVR (g) | ACVR (wt%) |
|---|---|---|---|---|---|
| HEMAVAC0.25 | 12.84 | 19.82 | 0.055 | 0.0123 | 0.25 |
| HEMAVAC0.50 | 12.84 | 19.82 | 0.055 | 0.0245 | 0.50 |
| HEMAVAC0.75 | 12.84 | 19.82 | 0.055 | 0.0368 | 0.75 |
| HEMAVAC1.00 | 12.84 | 19.82 | 0.055 | 0.0490 | 1.00 |
| HEMAVAC1.25 | 12.84 | 19.82 | 0.055 | 0.0613 | 1.25 |

### 3.4. Characterization

The structure of the prepared HEMAVA copolymer was characterized by FTIR and $^{1}$HNMR analysis, and the dispersion of the ACVR particles in the HEMAVAC composites was investigated by DSC, XRD and SEM analysis. The transparency of the specimens was examined by UV–visible light analysis, and the optical refractive index of these samples was determined using a collimated laser beam. The mechanical properties, which were based mainly on Young's modulus measurements of hydrated specimens, were studied in a micromechanical test. The cell toxicity and the cell adhesion were examined by LDH and MTT assays, respectively.

#### 3.4.1. FTIR Analysis

Fourier-transform infrared (FTIR) spectra of the samples were recorded on a Perkin Elmer Spectrum GX FTIR spectrometer operating in attenuated total reflection mode in a wave number range of 4000 to 650 $cm^{-1}$ for 32 cycles of scanning and at a resolution of 2 $cm^{-1}$. The samples were analyzed in the form of thin, transparent films deposited on dehydrated NaCl pallets.

#### 3.4.2. $^{1}$HNMR Analysis

The $^{1}$HNMR analysis of samples was carried out on a JEOL FX 90 Q NMR spectrometer at 500 MHz in deterred DMSO at room temperature.

3.4.3. DSC Analysis

The DSC thermograms of HEMAVA copolymer, ACVR drug and HEMAVAC composites were traced on a DSC device (Shimadsu DSC 60, Kyoto, Japan) previously calibrated with indium. Between 10 and 12 mg of samples was packaged in aluminum DSC capsules before being placed in the DSC cell. Samples were scanned by heating from −25 to 300 °C with a heating rate of 10 °C·min$^{-1}$. The value of the glass transition temperature ($T_g$) was taken from the inflection point of the thermal curves and the melting temperature of ACVR particles from the endothermic peak corresponding to the enthalpy of fusion of the sample.

3.4.4. XRD Analysis

The X-ray spectrographs of the samples were collected from an Advanced Bruker D8 diffractometer (Karlsruhe, Germany). Patterns were run with Cu Kα radiation at 40 mA and 40 kV with a 2θ scan rate of 2° min$^{-1}$.

3.4.5. SEM Analysis

The surface morphology of ACVR powder, dried thin films of HEMAVA and HEMAVAC with different ACVR contents coated with a gold grid was examined before and after the release process by scanning electron microscopic (SEM) using a Hitachi S4700 field emission scanning microscope (Tokyo, Japan).

3.4.6. UV–Visible Analysis

The ACVR amounts released from HEMAVAC drug carrier systems and the transparency of virgin HEMAVA and HEMAVAC thin films were determined by UV analysis using a UV–visible Ultrospec 2100 pro (Biosciences, Amersham, UK) spectroscope at 254 nm in water using an ACVR calibration curve.

3.4.7. Refractive Index Measurements

The specimen of the polymer, copolymer or composite was prepared directly by polymerization in a small cylindrical reactor, as shown in Scheme 3. A transparent, solid cylinder was obtained at the end of the reaction. The specimen was then allowed to air-dry for 72 h then in the vacuum oven at 40 °C for 24 h to remove any trace of residual monomers. The optical refractive index of the prepared specimens was determined using a collimated (1 mm diameter) laser beam illuminated by air on the side of the specimen and the recording of the optical path realized from the height of the cylinder. The angles of incidence, $\theta_{inc}$, and refraction, $\theta_{ref}$, as well as the index of refraction, $n$, of the sample were calculated using the Snell equation:

$$n = \frac{Sin\theta_{inc}}{Sin\theta_{ref}}, \quad (9)$$

In this application, three laser lamps of different wavelengths ranging from 405 to 670 nm were used to record the visible spectral range, and the value of the refractive index of each specimen was taken by calculating the arithmetic mean of three measurements. The dispersion curve of the refractive index between 400 and 800 nm was adjusted by means of the Cauchy relationship:

$$n(\lambda) = B + \frac{C}{\lambda^2}, \quad (10)$$

where $B$ and $C$ are empirical coefficients derived from the fit curve [59].

3.4.8. Mechanical Testing

The Young's modulus measurements of wet HEMAVA and wet HEMAVAC specimens were carried out on a micromechanical device of the DynacDalta tester type (Scientific Instruments (Bradford, UK)). Samples measuring 5 cm × 1 cm × 0.3 cm were attached from its ends by Luer-Lok handles specifically designed for this purpose and separated

at a rate of 0.5%·min$^{-1}$ for 15 s. The tensile force, $F$ (in grams), and the elongation of the specimen were calculated from the strain ($D$). The stress ($P$) applied to the specimen was determined from Equation (11) [39]:

$$P(kPa) = \frac{9.8 \times F}{S}, \quad (11)$$

where $S$ is the cross-section (in mm$^2$), which was accurately evaluated from the dimensions of the sample measured using an optical microscope. The apparent modulus of elasticity, E, of the specimens was directly deduced from the slope of the linear curve, indicating the change in content with elongation, as expressed by Equation (12) [39]:

$$(kPa) = \frac{P}{D} \times 100, \quad (12)$$

3.4.9. Wettability

The static water contact angles (WCA) were measured according to the procedure described by Wang et al. [60] using the sessile drop method on a contact angle analyzer (OCA 20, Dataphysics Instruments, Filderstadt, Germany). Briefly, the film samples were soaked in deionized water overnight until the swelling equilibrium was reached. After the free water on the surface of the hydrogel was removed gently by soft tissue paper, a drop of water was placed on the film sample surface, and the contact angle was immediately measured from the photo of the water drop. This experiment was triplicated, and the contact angle was taken from the average arithmetic values.

3.4.10. Swellability

The swelling degree measurement of the polymer sample was carried out at 37 °C in distilled water until saturation (swelling equilibrium). A square film sample of copolymer measuring 3 cm × 3 cm × 3 mm was completely immersed into a beaker containing 100 mL of distillated water. The whole was maintained under moderate agitation at a temperature of 37 °C. The specimen was then removed from the container at each time interval, and the droplets deposited on both surfaces of the film were gently wiped off using absorbent paper before being weighed on a precision balance. This experimentation was triplicated in the same conditions, and the swelling degree (S) was taken from the average arithmetic using Equation (13):

$$(wt\%) = \frac{w_t - w_o}{w_o} \times 100, \quad (13)$$

where $w_o$ and $w_t$ are the weights of the film sample before and at t time of the swelling process, respectively.

3.4.11. Cell Toxicity and Cell Adhesion

A—Cell toxicity by LDH assay

As described in one of our previous studies [61], the cellular cytotoxicity test was performed by LDH assay using the LDH Cytotoxicity Detection Kit. Briefly, a specimen containing 2 × 10$^5$ cells was seeded in 24-well plates for 24 h. A 50 µL amount of duplicate LDH mixture solution was added to an equivalent volume from each supernatant and was prepared in a 96-well plate and then incubated for 20 min at room temperature in the dark until the yellow color developed before reading at 490 nm with an iMark microplate absorbance spectrophotometer (Bio-Rad, Mississauga, ON, Canada). The cell toxicity was represented by percentage. Treated with 1% of Triton X-100, 2 × 10$^5$ cells were used as a positive control for LDH and corresponded to 100% of cytotoxicity. This experience was repeated three times.

B—Cell adhesion by MTT assay

Cell adhesion for each sample placed in 24-well plates was assessed using the MTT assay, as described by our previous work [62,63]. Cultured for adhesion overnight, $2 \times 10^5$ GMSMK cells/specimens were seeded in a 24-well plate. Then, 1/10 volume of 5 mg·mL$^{-1}$ MTT solution was added to each cell culture for 3 h incubation at 37 °C in the dark before lysing the cells with 300 µL of isopropanol and 0.05 N of HCL solution. To measure absorbance at 550 nm with an iMark reader (Bio-Rad, Mississauga, ON, Canada), $2 \times 100$ µL of lysed solution was transferred to a 96-well microplate. The percentage of viable proliferating cells was determined by % cell viability. Zero percent adhesion corresponded to absorbance (A) at 550 nm for a cell-free specimen.

#### 3.4.12. ACVR Solubility Improvement

The maximum solubility of ACVR in a medium with pH 7 was determined at 37 °C and shaken at 48 h using the shake-flask method [64]. The saturation of the ACVR–media solution was characterized by the beginning of turbidity appearance in which the absorbance in the UV–visible range rose sharply due to the reflectance of the insoluble ACVR particles. The saturated solution was immediately centrifuged at the same temperature using a micro-centrifuge RM-12C BL, and the supernatant liquid was filtered. Aliquots of 0.5 mL were withdrawn from the supernatant and diluted with the same media to prevent crystallization. The absorbance measurement was realized at 37 °C, and the maximum solubility of ACVR in neutral pH medium was taken from the average of three experimentations.

### *3.5. In Vitro Drug Release Studies*

HEMAVAC film samples with different ACVR contents were separately immersed in 20 mL of bi-distillated water maintained at a neutral pH, body temperature (37 °C) and at a stirring rate of 100 rpm for one week. To monitor ACVR released, aliquots of 0.5 mL were withdrawn at time intervals and immediately returned to the media just after analysis. This operation allowed a constant volume of media to be maintained during the release process. The total mass of ACVR released during a defined period was calculated from the standard absorbance curve, as mentioned above. It is important to note that, during the release process, the pH of water was practically unaffected by the small amount of ACVR released ($pKa_1$ = 2.16 and $pKa_2$ = 9.25) [65]; in this case, the addition of a buffer solution to water was not necessary.

## 4. Conclusions

The main objective of this work was achieved. Indeed, the poly(2-hydroxyethyl methacrylate-co-vinyl acetate)/acyclovir drug carrier system was successfully prepared by photo-polymerization of 2-hydroxyethyl methacrylate with vinyl acetate using a domestic LED lamp, and the properties studied showed that this material may be a potential candidate to be used as a contact lens regulating the release of acyclovir to the surface of the eye. The chemical structure of the prepared material was confirmed by spectroscopy analysis, and the uniform dispersion of the ACVR in the HEMAVA carrier in its molecular state was proved by the DSC, XRD and SEM methods. The transparency and the refractive index of the prepared lenses had properties comparable to those of poly(methyl methacrylate), largely used as contact lens, and the incorporation of between 0.5 and 1.25 wt% of acyclovir in this copolymer matrix practically did not affect these properties. The water content in the prepared material at equilibrium increased with the ACVR content in the copolymer and decreased the apparent Young's modulus without significantly affecting the percent yield. This led to a decrease in the release dynamic of this medication in the medium. The cytotoxicity test revealed no significant toxicity of the HEMAVA carrier, and the incorporation between 0.25 and 1.25 wt% ACVR in this copolymer did not affect the viability of the cell; thus, this system can be used as safe candidate for ACVR delivery from these prepared contact lenses. The diffusion of both water and ACVR through the HEMAVA matrix followed a Fickian model, and the dynamic release was easily controlled through the ACVR/HEMAVA ratio. The "in vitro" study of the ACVR released from the HEMAVAC drug carrier system in a neutral pH medium was satisfactory and promising because,

by changing the ACVR/HEMAVA ratio, this system was able to consistently deliver uniformly adequate amounts of ACVR over a long period (6 days). This process minimized the excess drug that is usually wasted when it is directly administered by the usual method. A 57.80 mol.% amount in VAc units in the copolymer made it possible to control the swelling capacity of this material in the medium through a compromise between the hydrophilic nature of HEMA and the hydrophobic character of VAc. This made it possible to control the quantity of ACVR released to a minimum and to regulate its release dynamic for one week.

**Author Contributions:** Conceptualization, R.S.A.K.; Data curation, S.M.A., R.S.A.K. and W.S.S.; Formal analysis, S.M.A., R.S.A.K., W.S.S., A.A. (Abeer Aljubailah), A.S. and T.A.; Drug, I.B. assisted S.M.A. and R.S.A.K. to investigate the drug release and its kinetics; A.A. (Amal Aldarwesh) encouraged T.A. to investigate the toxicicity and cell adhesion, S.M.A., R.S.A.K., M.A., A.A. (Abeer Aljubailah), A.S. and T.A.; Project administration, T.A.; Resources, S.M.A., M.A. and W.S.S.; Software, S.M.A., R.S.A.K., M.A. and W.S.S.; Supervision, T.A.; Writing—original draft, T.A.; Writing—review and editing, S.M.A., W.S.S. and T.A. All authors have read and agreed to the published version of the manuscript.

**Funding:** This research was funded by Researchers Supporting Project number (RSPD2023R 767), King Saud University, Riyadh, Saudi Arabia.

**Institutional Review Board Statement:** Not applicable.

**Informed Consent Statement:** Not applicable.

**Data Availability Statement:** The data presented in this study are available in the article.

**Acknowledgments:** The authors extend their appreciation to Researchers Supporting Project number (RSPD2023R 767), King Saud University, Riyadh, Saudi Arabia.

**Conflicts of Interest:** The authors declare no conflict of interest.

## References

1. Anderson, J.; Kim, S. Advances in drug delivery systems (3), book review. *J. Pharm. Sci.* **1989**, *78*, 608–609.
2. Heller, A. Integrated medical feedback systems for drug delivery. *AIChE J.* **2005**, *51*, 1054–1066. [CrossRef]
3. Langer, R.; Peppas, N.A. Advances in biomaterials, drug delivery, and bionanotechnology. *AIChE J.* **2003**, *49*, 2990–3006. [CrossRef]
4. Martinho, N.; Damgé, C.; Reis, C.P. Recent advances in drug delivery systems. *J. Biomater. Nanobiotechnol.* **2011**, *2*, 510. [CrossRef]
5. Chen, Y.; Li, J.; Lu, J.; Ding, M.; Chen, Y. Synthesis and properties of poly (vinyl alcohol) hydrogels with high strength and toughness. *Polym. Test.* **2022**, *108*, 107516. [CrossRef]
6. Lu, J.; Chen, Y.; Ding, M.; Fan, X.; Hu, J.; Chen, Y.; Li, J.; Li, Z.; Liu, W. A 4arm-PEG macromolecule crosslinked chitosan hydrogels as antibacterial wound dressing. *Carbohydr. Polym.* **2022**, *277*, 118871. [CrossRef]
7. Zare, M.; Bigham, A.; Zare, M.; Luo, H.; Rezvani Ghomi, E.; Ramakrishna, S. pHEMA: An overview for biomedical applications. *Int. J. Mol. Sci.* **2021**, *22*, 6376. [CrossRef]
8. Roberts, J.; Martens, P. Engineering biosynthetic cell encapsulation systems. In *Biosynthetic Polymers for Medical Applications*; Elsevier: Amsterdam, The Netherlands, 2016; pp. 205–239.
9. Sivalingam, G.; Chattopadhyay, S.; Madras, G. Enzymatic degradation of poly (ε-caprolactone), poly (vinyl acetate) and their blends by lipases. *Chem. Eng. Sci.* **2003**, *58*, 2911–2919. [CrossRef]
10. Novoa, G.A.G.; Heinämäki, J.; Mirza, S.; Antikainen, O.; Colarte, A.I.; Paz, A.S.; Yliruusi, J. Physical solid-state properties and dissolution of sustained-release matrices of polyvinylacetate. *Eur. J. Pharm. Biopharm.* **2005**, *59*, 343–350. [CrossRef]
11. Sung, J.H.; Hwang, M.-R.; Kim, J.O.; Lee, J.H.; Kim, Y.I.; Kim, J.H.; Chang, S.W.; Jin, S.G.; Kim, J.A.; Lyoo, W.S. Gel characterisation and in vivo evaluation of minocycline-loaded wound dressing with enhanced wound healing using polyvinyl alcohol and chitosan. *Int. J. Pharm.* **2010**, *392*, 232–240. [CrossRef]
12. Otto, W.; Drahoslav, L. Hydrophilic gels in biologic use. *Nature* **1960**, *185*, 117–118.
13. Sung, Y.; Gregonis, D.; John, M.; Andrade, J. Thermal and pulse NMR analysis of water in poly (2-hydroxyethyl methacrylate). *J. Appl. Polym. Sci.* **1981**, *26*, 3719–3728. [CrossRef]
14. Ferreira, L.; Vidal, M.; Gil, M. Evaluation of poly (2-hydroxyethyl methacrylate) gels as drug delivery systems at different pH values. *Int. J. Pharm.* **2000**, *194*, 169–180. [CrossRef]
15. Hsiue, G.-H.; Guu, J.-A.; Cheng, C.-C. Poly (2-hydroxyethyl methacrylate) film as a drug delivery system for pilocarpine. *Biomaterials* **2001**, *22*, 1763–1769. [CrossRef]
16. Hanak, B.W.; Hsieh, C.Y.; Donaldson, W.; Browd, S.R.; Lau, K.K.; Shain, W. Reduced cell attachment to poly (2-hydroxyethyl methacrylate)-coated ventricular catheters in vitro. *J. Biomed. Mater. Res. Part B Appl. Biomater.* **2018**, *106*, 1268–1279. [CrossRef]

17. Bailly, N.; Thomas, M.; Klumperman, B. Poly (N-vinylpyrrolidone)-block-poly (vinyl acetate) as a drug delivery vehicle for hydrophobic drugs. *Biomacromolecules* **2012**, *13*, 4109–4117. [CrossRef]
18. Schneider, C.; Langer, R.; Loveday, D.; Hair, D. Applications of ethylene vinyl acetate copolymers (EVA) in drug delivery systems. *J. Control. Release* **2017**, *262*, 284–295. [CrossRef]
19. Villanueva-Flores, F.; Miranda-Hernández, M.; Flores-Flores, J.O.; Porras-Sanjuanico, A.; Hu, H.; Pérez-Martínez, L.; Ramírez, O.T.; Palomares, L.A. Poly (vinyl alcohol co-vinyl acetate) as a novel scaffold for mammalian cell culture and controlled drug release. *J. Mater. Sci.* **2019**, *54*, 7867–7882. [CrossRef]
20. Jannesari, M.; Varshosaz, J.; Morshed, M.; Zamani, M. Composite poly (vinyl alcohol)/poly (vinyl acetate) electrospun nanofibrous mats as a novel wound dressing matrix for controlled release of drugs. *Int. J. Nanomed.* **2011**, *6*, 993–1003.
21. Donnenfeld, E.D. Oral Acyclovir for Herpes Simplex Virus Eye Disease. *Evid. Based Ophthalmol.* **2001**, *2*, 20–21. [CrossRef]
22. Group, H.E.D.S. Acyclovir for the prevention of recurrent herpes simplex virus eye disease. *N. Engl. J. Med.* **1998**, *339*, 300–306.
23. Luengo, J.; Aránguiz, T.; Sepúlveda, J.; Hernández, L.; Von Plessing, C. Preliminary pharmacokinetic study of different preparations of acyclovir with β-cyclodextrin. *J. Pharm. Sci.* **2002**, *91*, 2593–2598. [CrossRef] [PubMed]
24. Fox, T.G. Influence of diluent and of copolymer composition on the glass temperature of a polymer system. *Bull. Am. Phs. Soc.* **1952**, *1*, 123.
25. Patel, P.J.; Gohel, M.C.; Acharya, S.R. Exploration of statistical experimental design to improve entrapment efficiency of acyclovir in poly (d, l) lactide nanoparticles. *Pharm. Dev. Technol.* **2014**, *19*, 200–212. [CrossRef]
26. Yu, D.-G.; Zhu, L.-M.; Branford-White, C.J.; Yang, J.-H.; Wang, X.; Li, Y.; Qian, W. Solid dispersions in the form of electrospun core-sheath nanofibers. *Int. J. Nanomed.* **2011**, *6*, 3271–3280. [CrossRef]
27. Siddiqui, M.N.; Redhwi, H.H.; Tsagkalias, I.; Softas, C.; Ioannidou, M.D.; Achilias, D.S. Synthesis and characterization of poly (2-hydroxyethyl methacrylate)/silver hydrogel nanocomposites prepared via in situ radical polymerization. *Thermochim. Acta* **2016**, *643*, 53–64. [CrossRef]
28. Abdelghany, A.; Meikhail, M.; Asker, N. Synthesis and structural-biological correlation of PVC\PVAc polymer blends. *J. Mater. Res. Technol.* **2019**, *8*, 3908–3916. [CrossRef]
29. Khan, S.; Ranjha, N.M. Effect of degree of cross-linking on swelling and on drug release of low viscous chitosan/poly (vinyl alcohol) hydrogels. *Polym. Bull.* **2014**, *71*, 2133–2158. [CrossRef]
30. Numata, I.; Cochrane, M.A.; Souza Jr, C.M.; Sales, M.H. Carbon emissions from deforestation and forest fragmentation in the Brazilian Amazon. *Environ. Res. Lett.* **2011**, *6*, 044003. [CrossRef]
31. Aso, Y.; Yoshioka, S.; Po, A.L.W.; Terao, T. Effect of temperature on mechanisms of drug release and matrix degradation of poly (d, l-lactide) microspheres. *J. Control. Release* **1994**, *31*, 33–39. [CrossRef]
32. Aydin, N.E. Effect of temperature on drug release: Production of 5-FU-encapsulated hydroxyapatite-gelatin polymer composites via spray drying and analysis of in vitro kinetics. *Int. J. Polym. Sci.* **2020**, *2020*, 8017035. [CrossRef]
33. Akula, P.; PK, L. Effect of pH on weakly acidic and basic model drugs and determination of their ex vivo transdermal permeation routes. *Braz. J. Pharm. Sci.* **2018**, *54*, e00070. [CrossRef]
34. Aljubailah, A.; Alharbi, W.N.O.; Haidyrah, A.S.; Al-Garni, T.S.; Saeed, W.S.; Semlali, A.; Alqahtani, S.; Al-Owais, A.A.; Karami, A.M.; Aouak, T. Copolymer Involving 2-Hydroxyethyl Methacrylate and 2-Chloroquinyl Methacrylate: Synthesis, Characterization and In Vitro 2-Hydroxychloroquine Delivery Application. *Polymers* **2021**, *13*, 4072. [CrossRef]
35. Nicolson, P.C.; Vogt, J. Soft contact lens polymers: An evolution. *Biomaterials* **2001**, *22*, 3273–3283. [CrossRef]
36. Comyn, J. Introduction to polymer permeability and the mathematics of diffusion. In *Polymer Permeability*; Springer: Dordrecht, The Netherlands, 1985; pp. 1–10. [CrossRef]
37. Masaro, L.; Zhu, X. Physical models of diffusion for polymer solutions, gels and solids. *Prog. Polym. Sci.* **1999**, *24*, 731–775. [CrossRef]
38. Varikooty, J.; Keir, N.; Woods, C.A.; Fonn, D. Measurement of the refractive index of soft contact lenses during wear. *Eye Contact Lens* **2010**, *36*, 2–5. [CrossRef]
39. Luo, Y.; Dalton, P.D.; Shoichet, M.S. Investigating the properties of novel poly (2-hydroxyethyl methacrylate-co-methyl methacrylate) hydrogel hollow fiber membranes. *Chem. Mater.* **2001**, *13*, 4087–4093. [CrossRef]
40. Bhamra, T.S.; Tighe, B.J. Mechanical properties of contact lenses: The contribution of measurement techniques and clinical feedback to 50 years of materials development. *Contact Lens Anterior Eye* **2017**, *40*, 70–81. [CrossRef]
41. Horst, C.R.; Brodland, B.; Jones, L.W.; Brodland, G.W. Measuring the modulus of silicone hydrogel contact lenses. *Optom. Vis. Sci.* **2012**, *89*, 1468–1476. [CrossRef]
42. Ishiyama, C.; Higo, Y. Effects of humidity on Young's modulus in poly (methyl methacrylate). *J. Polym. Sci. Part B Polym. Phys.* **2002**, *40*, 460–465. [CrossRef]
43. Vargün, E.; Sankir, M.; Aran, B.; Sankir, N.D.; Usanmaz, A. Synthesis and characterization of 2-hydroxyethyl methacrylate (HEMA) and methyl methacrylate (MMA) copolymer used as biomaterial. *J. Macromol. Sci. Part A Pure Appl. Chem.* **2010**, *47*, 235–240. [CrossRef]
44. Final Report on the Safety Assessment of Polyvinyl Acetate. *J. Am. Coll. Toxicol.* **1992**, *11*, 465–473. [CrossRef]
45. Liu, X.; Wang, C.-H.; Dai, C.; Camesa, A.; Zhang, H.F.; Jiao, S. Effect of contact lens on optical coherence tomography imaging of rodent retina. *Curr. Eye Res.* **2013**, *38*, 1235–1240. [CrossRef] [PubMed]
46. Campbell, D.; Carnell, S.M.; Eden, R.J. Applicability of contact angle techniques used in the analysis of contact lenses, part 1: Comparative methodologies. *Eye Contact Lens* **2013**, *39*, 254–262. [CrossRef]

47. Toledo, E.J.; Ramalho, T.C.; Magriotis, Z.M. Influence of magnetic field on physical–chemical properties of the liquid water: Insights from experimental and theoretical models. *J. Mol. Struct.* **2008**, *888*, 409–415. [CrossRef]
48. Weber, M.J. *Handbook of Optical Materials*; CRC Press: Boca Raton, FL, USA, 2018.
49. Reinhard, C.S.; Radomsky, M.L.; Saltzman, W.M.; Hilton, J.; Brem, H. Polymeric controlled release of dexamethasone in normal rat brain. *J. Control. Release* **1991**, *16*, 331–339. [CrossRef]
50. Cypes, S.H.; Saltzman, W.M.; Giannelis, E.P. Organosilicate-polymer drug delivery systems: Controlled release and enhanced mechanical properties. *J. Control. Release* **2003**, *90*, 163–169. [CrossRef]
51. Frank, A.; Rath, S.K.; Venkatraman, S.S. Controlled release from bioerodible polymers: Effect of drug type and polymer composition. *J. Control. Release* **2005**, *102*, 333–344. [CrossRef]
52. Dilmi, A.; Bartil, T.; Yahia, N.; Benneghmouche, Z. Hydrogels based on 2-hydroxyethylmethacrylate and chitosan: Preparation, swelling behavior, and drug delivery. *Int. J. Polym. Mater. Polym. Biomater.* **2014**, *63*, 502–509. [CrossRef]
53. Kim, S.K. Small intestine transit time in the normal small bowel study. *Am. J. Roentgenol.* **1968**, *104*, 522–524. [CrossRef]
54. Lee, Y.Y.; Erdogan, A.; Rao, S.S. How to assess regional and whole gut transit time with wireless motility capsule. *J. Neurogastroenterol. Motil.* **2014**, *20*, 265. [CrossRef]
55. Wan, L.S.; Heng, P.W.; Wong, L.F. Relationship between swelling and drug release in a hydrophilic matrix. *Drug Dev. Ind. Pharm.* **1993**, *19*, 1201–1210. [CrossRef]
56. Khalid, S.; Qadir, M.; Massud, A.; Ali, M.; Rasool, M. Effect of degree of cross-linking on swelling and drug release behaviour of poly (methyl methacrylate-co-itaconic acid)[P (MMA/IA)] hydrogels for site specific drug delivery. *J. Drug Deliv. Sci. Technol.* **2009**, *19*, 413. [CrossRef]
57. Dinu-Pirvu, C.; Ivana, S. A study of the influence of crosslinking degree on the physicochemical properties of gelatin microparticles. *Cellul. Chem. Technol.* **2013**, *47*, 721–726.
58. Carbinatto, F.M.; de Castro, A.D.; Evangelista, R.C.; Cury, B.S. Insights into the swelling process and drug release mechanisms from cross-linked pectin/high amylose starch matrices. *Asian J. Pharm. Sci.* **2014**, *9*, 27–34. [CrossRef]
59. Bonal, V.; Quintana, J.A.; Villalvilla, J.M.; Muñoz-Mármol, R.; Mira-Martínez, J.C.; Boj, P.G.; Cruz, M.E.; Castro, Y.; Díaz-García, M.A. Simultaneous determination of refractive index and thickness of submicron optical polymer films from transmission spectra. *Polymers* **2021**, *13*, 2545. [CrossRef]
60. Wang, Z.; Li, X.; Zhang, X.; Sheng, R.; Lin, Q.; Song, W.; Hao, L. Novel contact lenses embedded with drug-loaded Zwitterionic nanogels for extended ophthalmic drug delivery. *Nanomaterials* **2021**, *11*, 2328. [CrossRef]
61. Semlali, A.; Papadakos, S.; Contant, C.; Zouaoui, I.; Rouabhia, M. Rapamycin inhibits oral cancer cell growth by promoting oxidative stress and suppressing ERK1/2, NF-κB and beta-catenin pathways. *Front. Oncol.* **2022**, *12*, 873447. [CrossRef]
62. Alghamdi, A.A.; Saeed, W.S.; Al-Odayni, A.-B.; Alharthi, F.A.; Semlali, A.; Aouak, T. Poly (ethylene-co-vinylalcohol)/poly (δ-valerolactone)/aspirin composite: Model for a new drug-carrier system. *Polymers* **2019**, *11*, 439. [CrossRef]
63. Alghamdi, A.A.; Alsolami, A.; Saeed, W.S.; Al-Odayni, A.-B.M.; Semlali, A.; Aouak, T. Miscibility of poly (acrylic acid)/poly (methyl vinyl ketone) blend and in vitro application as drug carrier system. *Des. Monomers Polym.* **2018**, *21*, 145–162. [CrossRef]
64. Baka, E.; Comer, J.E.; Takács-Novák, K. Study of equilibrium solubility measurement by saturation shake-flask method using hydrochlorothiazide as model compound. *J. Pharm. Biomed. Anal.* **2008**, *46*, 335–341. [CrossRef] [PubMed]
65. Arnal, J.; Gonzalez-Alvarez, I.; Bermejo, M.; Amidon, G.L.; Junginger, H.; Kopp, S.; Midha, K.K.; Shah, V.; Stavchansky, S.; Dressman, J.B. Biowaiver monographs for immediate release solid oral dosage forms: Aciclovir. *J. Pharm. Sci.* **2008**, *97*, 5061–5073. [CrossRef] [PubMed]